Published in final edited form as:

*Magn Reson Med*. 2018 March ; 79(3): 1266–1275. doi:10.1002/mrm.26811.

# Metabolic Assessment of a Migraine Model using Relaxation-Enhanced $^{1}$H Spectroscopy at Ultra-High Field

**Nastaren Abad**[a,b], **Jens T. Rosenberg**[b], **Tangi Roussel**[c], **Dillon C. Grice**[a], **Michael G. Harrington**[d,†], and **Samuel C. Grant**[a,b,†]

[a]Department of Chemical and Biomedical Engineering, FAMU-FSU College of Engineering, Tallahassee, FL, USA

[b]The National High Magnetic Field Laboratory, Florida State University, Tallahassee, FL, USA

[c]Department of Chemical Physics, Weizmann Institute Science, Rehovot 76100, Israel

[d]Molecular Neurology Program, Huntington Medical Research Institutes, Pasadena, CA, USA

## Abstract

**Purpose—**This study evaluates biochemical imbalances in a rat model that reflects dysfunctional pathways in migraine. The high sensitivity and spectral dispersion available to $^{1}$H MRS at 21.1 T expands metabolic profiling in this migraine model to include lactate (Lac), taurine (Tau), aspartate (Asp) and Gly—a mixture of glycine, glutamine and glutamate.

**Methods—**Sprague-Dawley male rats were administered *in situ* an intra-peritoneal injection of nitroglycerin (NTG) to induce the migraine analogue or saline as a control. A selective relaxation-enhanced MR spectroscopy (RE-MRS) sequence was utilized to target upfield metabolites from a $(4\text{-mm})^3$ voxel for 2.5 h post-injection.

**Results—**Significant increases were evident for Lac as early as 10 min post NTG injection, peaking over 50% compared to baseline and control (Normalized Lac/NAA with NTG=1.54±0.65 vs. with saline=0.99±0.08). Tau decreased in controls progressively over 2 h post-injection, but remained elevated with NTG, peaking at 105 min post-injection (Normalized Tau/NAA with NTG=1.10±0.18 vs. with saline=0.85±0.14). tCr under NTG showed significant decreases with time and compared to saline; Gly demonstrated temporal increases for NTG.

**Conclusions—**These changes indicate an altered metabolic profile in the migraine analogue consistent with early changes in neural activity and/or vasodilation consistent with progressively enhanced neuroprotection and osmoregulation.

### Keywords

Migraine; Nitroglycerin; $^{1}$H MR Spectroscopy; High Magnetic Field; Lactate; Taurine

**Corresponding Author:** Samuel C. Grant, National High Magnetic Field Laboratory (NHMFL), Center for Interdisciplinary Magnetic Resonance, 1800 E Paul Dirac Drive, Tallahassee, FL 32310, grant@magnet.fsu.edu.
[†]Co-senior authors

**Declaration of competing interests**
None

## Introduction

Migraines affect approximately 38 million people in the United States, and are the 7th most disabling condition in the world as assessed by interference with the sufferer's ability to function in everyday activities (1). Though several hypotheses implicate neuronal and trigeminovascular involvement with migraine onset and progression (2), an exact pathophysiological change is yet to be identified that can explain the onset, progression and termination of migraines.

Biochemical imbalances of $Na^+$ in migraine have been identified in the cerebrospinal fluid (CSF) (3,4), brain (5) and alterations of $Ca^{2+}$ and $Na^+$ channels as well as the $Na^+/K^+$/ ATPase transporter (NKAT) for the rare familial hemiplegic migraine mutation (6). However, there is limited characterization of metabolic changes during the onset and progression of migraine. It follows that the identification of specific metabolic changes may improve understanding of migraine and open new avenues for therapy development. This study, therefore, evaluates biochemical and metabolic imbalances hypothesized to reflect dysfunctional pathways paralleling migraine impacts in humans by means of a frequently studied nitroglycerin (NTG) triggered animal migraine model (5, 7–9). In clinical cohorts, NTG typically triggers a mild headache that is short-lived and stops rapidly after administration is completed, based on a short (2-min) half-life (10, 11). This mild, immediate headache results from the acute effects of nitric oxide (NO) as a vasodilator impacting the intra- and extracranial vasculature. For migraineurs, however, NTG triggers a delayed onset of central sensitization due to the action of NO on neuronal firing that is not observed in non-migraineurs. This sensitization is reflected in the animal analogue.

To probe metabolic imbalances resulting from NTG exposure, *in vivo* proton magnetic resonance spectroscopy ($^1$H MRS) is employed in this study to assess metabolic dysfunctions reflected in the dynamic concentrations of energetics, osmolytes and neurotransmitters. In previous studies at lower magnetic fields and in the occipital and temporoparietal regions, various metabolites have been interrogated with respect to migraine in patient populations: N-acetyl aspartate (NAA) (12); total creatine (tCr)—which includes phosphocreatine and creatine (13); total choline (Cho) (13); and Glx/GABA+, which is a mixture of spectral overlaps from GABA, glutamate and glutamine (14). Decreased levels of NAA, Cho and tCr indicate a potential impact of migraine on chronic neuronal integrity and decreased membrane turnover. However, these studies were conducted during the interictal period, and no clinical study to date has acquired $^1$H MRS during migraine. Preclinically, Ma and co-workers (15) made use of a migraine rodent model in their spectroscopy based study to evaluate metabolites. However, their study was performed at one time point 90 min after establishing the onset of the migraine analogue based on behavioral characterization. Additionally, their voxels were localized in the thalamus and cerebellum, and the primary metabolites interrogated were GLX/GABA+, creatine, choline, NAA and myoinositol (mI). Thus, several MRS studies have reported metabolic changes in migraine patients, but study designs and results have been heterogeneous, with little consistency between findings for $^1$H MRS (16, 17).

Leveraging the sensitivity and spectral dispersion benefits of high-field MRS, the overall aim of the present study is to interrogate metabolites at 21.1 T dynamically and *in vivo* during acute and delayed onset of central sensitization. To enhance sensitivity while reducing individual experiment acquisitions times, relaxation-enhanced MR spectroscopy (RE-MRS) was employed to analyze quantitative changes in brain metabolites during progression of the migraine analogue from baseline. RE-MRS utilizes specifically designed RF pulses to excite metabolites of known chemical shifts over a narrow bandwidth (18, 19). Through bandwidth selection that avoids the excitation of bulk $H_2O$, RE-MRS yields high fidelity spectra without water suppression while enhancing sensitivity and acquisition time efficiency by minimizing $T_1$ exchange issues associated with conventional *in vivo* spectroscopy.

For this study, the high sensitivity and spectral dispersion available to $^1H$ RE-MRS at 21.1 T expanded metabolic profiling in an animal model of migraine to include lactate (Lac), taurine (Tau), aspartate (Asp) and Gly, which was identified as a mixture of glycine, glutamine and glutamate. These substrates should provide insight into the impacts of acute migraine on energetics (tCr, Gly) and glycolysis (Lac, Asp) as well as neuroprotective and osmoregulatory mechanisms (Tau) that may be instituted as a result of increased neurotransmitter (Glx, Gly) or homeostatic imbalances. Behaviorally, previous research has established that the first noticeable central sensitization in the rat model is evident at one hour after the NTG trigger and plateaus over the next four hours (5, 15); building upon this foundation, acquisitions in the present study were focused on a novel time course of metabolic regulation for acute (< 45 min) and delayed changes (> 45 min). Therefore, the present study evaluates $^1H$ MRS data acquired during the onset and progression in a rat model of acute migraine as a means of temporally mapping energetic and osmotic changes over a two-hour period following intraperitoneal (IP) injection of NTG.

## Methods

### Animal Models

Animal procedures were approved by the Institutional Animal Care and Uses Committees at the Florida State University in Tallahassee, FL and the Huntington Medical Research Institutes (HMRI) in Pasadena, CA.

While in the MRI scanner, a total of 17 Sprague-Dawley male rats (Harlan, Indianapolis, IN), weights between 170 and 250 g, were administered *in situ* an IP injection of either 10 mg/kg of NTG (n=11) to induce central sensitization or saline (n=6) as a control. For a dose of 10 mg/kg IP, the clinical NTG formulation contains 30% ethanol and 30% propylene glycol made up in normal saline (0.9% sodium chloride injection, USP, Baxter Healthcare Corporation, Deerfield, IL) at 7.4 pH. There is considerable evidence that the administration of nitric oxide (NO) donors, such as NTG, in humans induces headaches similar to those in migraine attacks (11, 20). As such, NTG-induced sensitization is a widely accepted migraine model in rodents (5,7–9), as well as humans (10). In preclinical models, NTG causes allodynia and hyperalgesia (21), brain sodium elevation and activation of cFos in the trigeminal nucleus caudalis neurons (TNC) (5), and abnormalities in the brain stem auditory evoked potentials of rats (7).

Animals were treated under anesthesia with the same procedure that consistently has demonstrated behavioral (aversive threshold and eye squinting) responses to NTG in unanesthetized rats and *ex vivo* cFos activation in the second order trigeminal neurons of the brainstem (5). For this study, rats were induced with 4% isoflurane in $O_2$ and maintained at 3% during surgical implantation of the IP line. During scanning, animals were maintained at approximately 2.5–1.5%, adjusted to retain a level plane of anesthesia while in the magnet. For imaging in a vertical 21.1-T magnet, rats were loaded into the RF coil and animal cradle in a supine position, and were positioned in a heads-up orientation during all scans. Respiratory rate was monitored (SA Instruments, Stony Brook, NY) and maintained between 30–50 breaths/min. The animals were kept at a constant temperature (26° C) in the MRI scanner by means of a regulated water supply. Animals were euthanized after experimentation.

## MRI/S Protocol

All scans were performed at the 21.1-T, 900-MHz vertical MRI scanner designed and constructed at the National High Magnetic Field Laboratory in Tallahassee, FL (22). The magnet is equipped with a Bruker Avance III console (Bruker-Biospin, Billerica, MA) and is operated using Paravision 5.1. A microimaging gradient system (Resonance Research, Inc., Billerica, MA) provides a peak gradient strength of 60 G/cm over a 64-mm diameter. For both excitation and detection, a homebuilt $^1$H radio frequency (RF) coil based on a linear birdcage design (23) was used to acquire *in vivo* $^1$H MRS.

Relaxation-Enhanced MRS (RE-MRS) was used to achieve selective spectral excitations for voxel sizes of $(4\ mm)^3$, without water suppression, to target upfield metabolites. In contrast to Shemesh *et al.* (19), the RE-MRS sequence was acquired with pulses selectively exciting and refocusing a broader band to achieve spectral information from more metabolites. Employing a spin-echo acquisition scheme, this selective excitation was accomplished with a 5-ms 10-lobe, hyperbolic sinc-shaped pulse (BW = 4095 Hz), and a 5-ms 180° refocusing pulse derived from the Shinnar-LeRoux algorithm (SLR), exciting a band between 0–4 ppm without touching the water resonance. As such, the bulk water pool acts as a sink into which metabolite protons can exchange without penalty against the more efficient and shorter $T_1$ values of metabolites (19, 24). These off-resonance pulses improve sensitivity by means of maintaining shorter metabolic $T_1$s and permitting for reduced repetition and acquisition times. Though not evaluated here, previous studies have demonstrated that *in vivo* RE-MRS maintains long metabolic $T_2$ (>100 ms), even under pathological conditions (19, 24). As such, this technique allows for the acquisition of high fidelity spectra over short acquisition times (~6 s for a single average) while maintaining high *in vivo* signal-to-noise ratios (> 50:1) at 21.1 T (19, 24). 3D spectroscopic localization was achieved using six 5-ms adiabatic pulses with localization by an adiabatic selective refocusing (3D LASER) approach (25). The echo time (TE) of the RE-MRS spin echo was 52 ms, which with the LASER module, yielded a total TE of 64 ms. Using a spectral width of 15 kHz and 4096 complex points, a repetition time (TR) of 2500 ms with 256 averages resulted in a total scan time of 10 min per scan. A total of 14 scans were acquired successively starting from pre-injection to ~2.5-h post injection, which allowed for investigation of metabolic properties during the onset and progression of central sensitization.

The voxel was localized in the right cerebral region encompassing a portion of the neocortex, corpus callosum and hippocampus, as demonstrated in Figure 1A. Despite the significant heterogeneity in terms of voxel localization in the human studies, previous studies have used a similar, mostly cortical voxel localization (13, 14). The selection, in this study, was based partially on the homogeneity of the rat brain relative to the voxel volume and a desire to investigate the impacts of the trigeminal afferent extensions into the cortex. The placement of each voxel was identified by making use of fast spin-echo localizers generated with spin echo Rapid Acquisition with Relaxation Enhancement (RARE) sequences. Considerable effort was made to create a homogenous $B_0$ field by a combination of automatic shim adjustment for linear, $1^{st}$ order shims and manual adjustment of higher order shims based on the water signal acquired from the $(4\text{-mm})^3$ voxel of interest. Although this *in vivo* voxel constituted a large volume evaluated at 21.1 T for a free breathing anesthetized rat, a nominal full width at half maximum of 40 Hz for all scans, with frequency linewidths achieved in the 32–35 Hz range.

## Data Analysis and Statistical Tests

Data was acquired as a partial echo, and magnitude spectra were generated after apodization (10-Hz exponential line broadening) and Fourier transform. The spectra upfield of water contains important resonances including, but not limited to mI, Gly, Glx, Tau, tCr, Cho, Asp, NAA and Lac. These substrates are involved in cellular metabolism, with at least half of the metabolites specific to the CNS. The *in vivo* assignments of these peaks were based on the resonances identified in the Human Metabolome Database (26), and they are labeled on the representative spectra of Figure 1B. For spectra quantification, both peak height and integral were calculated for the above metabolites at the chemical shifts indicated in Figure 1B. In both quantification approaches, a 10-point (<75 Hz) range was permitted to account for any variability in the peak assignment. With respect to change over time, no significant differences were identified between integral and peak height measurements; data are reported subsequently based on peak height measurements to minimize the impact of adjacent resonant peaks or potential macromolecular baseline irregularities on the metabolites of interest. No modeling or deconvolution of spectral components was performed. Data were plotted as a function of time pre- and post-injection to develop a time course of metabolic changes.

This raw data time course was normalized to the NAA peak (found experimentally to be stable for NTG and saline over all data points) and was further referenced to the pre-injection baseline. Individual time points from all animals in the NTG and saline groups based on these time series were averaged to determine trends and significance. All datasets were analyzed using IBM SPSS 20.0 for Windows (SPSS Inc., Chicago, IL, USA). The NAA-normalized intensities for each metabolite and from each scan of the time series were analyzed by means of a mixed model ANOVA with repeated measures to conduct *within* subject analysis. A least significant difference (LSD) post hoc test was applied for pairwise comparisons between time points, with $p<0.05$ deemed significant for temporal assessments within a group (NTG or saline). To assess *between* group effects, a multivariate ANOVA was applied to the same data normalized to the pre-injection ratio, with a Bonferroni's post hoc test used for comparisons between NTG and saline cohorts; changes between groups were

deemed significant for $F(1,14) = 4.60$, $p<0.05$. This statistical approach allowed for multiple dependent (temporal effects) and independent (NTG vs. saline) variables to be analyzed. The normality and variance of the data were assessed as part of the ANOVA. Based on the Shapiro-Wilks W and Levene's tests of the ANOVA, metabolic data met normality and sphericity requirements to justify these statistical tests.

## Results

Figure 1 demonstrates the time course of metabolite signal changes relative to pre-injection levels in the NTG administered models (1C), which coincides with the established onset and progression of central sensitization using the same protocol (5), versus the saline administered controls (1D). As is evident, the RE-MRS sequence provides high fidelity data with flat baselines while avoiding the water resonance through the selective excitation of the targeted metabolites upfield of the bulk water resonance. This high quality *in vivo* spectra and signal enhancement resulting from reduced chemical exchange impacts (and lack of subsequent $T_1$ lengthening) with bulk water allows for accurate peak assignment and characterization of these resonances as biomarkers for this migraine analogue. To demonstrate stability and selective metabolic increases, difference spectra are provided in Supporting Figures S1 and S2.

The effect of NTG on the individual metabolites is shown in Figures 2–6. The major changes are observed in Lac (Figure 2) and Tau (Figure 3), with lesser impacts to tCr (Figure 4), demonstrating differential acute and delayed onset impacts in response to NTG compared to the control (saline-injected) group. At 10 min post-injection, the first to change is Lac, which remains elevated 85 min after NTG administration. Significant increases in Lac were evident as early as 10 min post NTG administration, and achieved a peak value of over 50% compared to the baseline and controls at 35 min post injection. At this peak, normalized Lac/NAA values with respect to NTG had a mean ± standard deviation of 1.54±0.65 compared to saline injection, which achieved a mean of 0.99±0.08.

Tau relative levels decrease progressively through 2 h in saline controls, whereas, they remain level or with modest increase in the NTG treated rats. Tau values peaked at 105 min post injection with a percent difference of 26% between the NTG injected and saline cohorts. At its peak, normalized Tau/NAA values for the NTG group had a mean of 1.10±0.18 compared to the saline injected cohorts, which had decreased to 0.85±0.14 from baseline.

In contrast, Cho (Figure 5) in the NTG group remains consistent with the values from the saline controls, although both NTG and saline groups display overall decreases in Cho with time. Conversely, an interesting trend is evident in the profile presented by Gly (Figure 6), which demonstrates a delayed increase that becomes more pronounced, possibly corresponding to the onset of central sensitization. Data for Glx and Asp was measured but their concentrations remained unaltered in NTG and saline treated animals (see Supporting Figures S3 and S4).

## Discussion

The present study offers insight into *in vivo* metabolic fluxes in the brain with the onset and progression of an acute migraine analogue in rodents. Significant changes in Lac, Tau and tCr levels between the migraine (NTG-triggered) analogue and control (saline-injected) animals are evident as a function of time post injection. Other metabolites demonstrated no difference between these treatment groups, with the possible exception of Gly, which displayed a modest increasing trend and delayed significance for temporal and between-group comparisons for NTG-exposed rats versus saline controls. Uniquely, these metabolites have not been evaluated previously in an *in vivo* rodent migraine model on a time course basis that spans both acute and delayed onset of' NTG-triggered central sensitization. The time-dependent altered levels of Lac, tCr, Tau and potentially Gly may prove to be important biomarkers of migraine onset.

The significant increase in Lac indicates a transient effect from increased neural activity and a move towards either anaerobic respiration or compromised aerobic respiration in the brain, which gradually returns to baseline values. Lactate is well known as an end-product of anaerobic glycolysis (35); however, brain lactate produced through aerobic glycolysis (36) is constantly present in spite of adequate oxygenation, and local increases in neural activity rapidly and transiently elevate lactate levels (37). Moreover, lactate release and glucose uptake in astrocytes were stimulated by sodium-coupled uptake of glutamate (38), and elevated lactate previously was found to suppress neuronal firing in the hippocampus (39). Notably, four clinical $^{1}$H MRS studies (27–29, 40) have reported increased Lac during the interictal period of chronic migraineurs compared to age-matched controls but other studies (33, 41–44) did not achieve significant Lac changes. Elevated Lac levels were reported in the occipital cortex by Watanabe *et al.* (27) and Sandor *et al.* (28), in the cerebellum of the FHMII mutation in migraine by Grimaldi and co-workers (29) and in the thamalus by Mohamed *et al.* (40). These authors attributed higher Lac levels to increased glycolytic activity due to impaired oxidative metabolism and mitochondrial dysfunction in chronic migraineurs. However, other groups (13, 17) did not observe the same Lac changes among their human subjects, possibly due to low limits of detection. More consistently, the most reproducible findings of human $^{31}$P MRS studies of migraine are concomitantly decreased PCr and increased inorganic phosphate (16), with additional studies independently reporting decreased phosphorylation potential (31–34). These findings suggest a chronic reduction in the availability of free cellular energy in migraineurs and possible mitochondrial dysfunction (30), which may be related to the disturbed energy metabolism in the NTG rats. Thus, the striking and early metabolic change in brain Lac during onset and progression in the current study is at least indicative of short-term metabolic remodeling and is worthy of further study, both in clinical migraine and preclinical models.

Significant decreases in tCr levels also were evident in NTG-treated rats compared to controls. Although at maximum only a 3% difference compared to baseline, NTG treatment consistently elicited a decrease in tCr as opposed to saline. Although more study is required, the decrease in tCr may be evidence of: the depletion of creatine and/or phosphocreatine from the cerebral voxel under investigation—a result of energy requirements elsewhere in the sensitized brain; the uptake of creatine as a compensatory osmolyte by cells experiencing

osmotic stress—a neuroprotective function that may also be represented in elevated Tau (45); or inhibition of endogenous creatine synthesis by glial cells in the cortex (46). Most clinical $^{1}$H MRS studies do not identify tCr changes (16); however, a 3-year, longitudinal study (47) did identify a small decrease in tCr during interictal periods, which was attributed to reduced glial cellularity and energy production. Taken together, the decrease in tCr and increase in Lac represent a potential remodeling of metabolic processes related to energetics under the influence of acute central sensitization.

Of additional interest were the increased levels of Tau and, to a lesser extent, Gly in the migraine analogue compared to controls. Elevated levels of Gly have been reported (48–50) in the CSF in migraine, and it is interesting that a similar trend is replicated in the cerebral region of the rat brain after NTG administration. Previously, Tau levels were found to be elevated in CSF in migraine (49, 51); however, to the best of our knowledge, brain Tau levels have not been interrogated previously *in vivo* in migraine or animal models.

Taurine (2-Aminoethane Sulfonic acid), or Tau, is one of the most abundant amino acids found in mammals (52). Physiochemically, the sulfonic group (compared to carboxyl group on other amino acids) allows it a higher dissociation rate, with higher water solubility and low lipophilicity (52, 53). Biochemically, the distribution of Tau is ubiquitous, with higher levels reported in the muscles, brain and heart compared to plasma and CSF (52). Though Tau is touted to modulate a wide range of activities, its osmoregulatory and neuroprotective properties are the most pertinent within the scope of this study. The current findings demonstrate consistently lower Tau levels in controls over the time course of this study, while the relatively higher levels of Tau after NTG administration arise in the same time frame as the cortical vasodilation from NTG (54). Given the expected time course of the migraine analogue onset at greater than 45 min post NTG injection (8, 15), elevated Tau levels beginning and continuing past the 45-min mark can be attributed to the initial role of Tau in vasoregulation, but also its osmoregulatory and neuroprotective function on brain tissue.

The presence and effects of Tau have been studied in a wide variety of disease and disorder states, including but not limited to epilepsy, Alzheimer’s Disease, cardiovascular disorders and alcoholism (55). In cases of oxidative stress, Tau is considered to improve mitochondrial functioning by modulating the electron transport chain and impeding the generation of oxygen reactive species in hepatocytes (53). Taranukhin and co-workers (56) suggested the possibility of Tau counteracting alterations of membrane properties, including but not limited to the activity of NKAT. The phospholemman subunit of the NKAT regulates taurine efflux (57), thus meriting further study of Tau regulation in the migraine model.

Previously, Harrington and co-workers (58) had hypothesized the possibility of abnormally high activation of sodium transporters in migraineurs, with NKAT being the main exporter and thereby consuming almost half of normal brain’s energy in the maintenance of the sodium gradient (59). This hypothesis was based on findings of increased CSF sodium in migraineurs (4), supported by enhanced excitability of cultured hippocampal neurons exposed to increased extracellular sodium concentrations (21), and demonstrated by increased and sustained cranial sodium as assessed by $^{23}$Na MRI signal at 21.1 T in the

NTG-injected rat (5). Alterations in $Na^+$ homeostasis during migraine potentially lead to the increased and sustained levels of Tau, which in turn impacts membrane permeability via an osmoregulatory mechanism coupled to excess extracellular $Na^+$. Corresponding well with the established time for behavioral change of 45 min following NTG injection, the delayed and sustained increases in Tau for the migraine analogue rats could be indicative of its release kinetics, subsequent osmotic action and re-stabilization of NKAT function (52, 60, 61). The findings from Lac and tCr appear to be indicative of altered and redistributed energy metabolism, possibly arising from an anatomically-specific combination of increased energy consumption. Supporting the protective action of Tau and its time course, the immediate increases in Lac and decreases in tCr may be tied to increased localized energetic needs resulting from enhanced neural and NKAT activity prior to and continuing through the onset of central sensitization.

The present study found an increasing trend in Gly, supporting either altered states of metabolism, stimulation and/or neuroprotection. Interestingly, Glx appeared unaltered with the onset and progression of central sensitization. Being a combination of excitatory and inhibitory neurotransmitters, Glx metabolites are involved in the modulation of pain and neuronal excitability (14). Taken together, the Gly trend and Glx stability hints that the potential increase in Gly may arise more from glycine, which could be attributable to changes in glycolysis that occur prior to pain. However, the current study could not resolve the spectral overlap of GABA, glutamate and glutamine in Glx or of glycine, glutamine and glutamate in Gly, leading to some ambiguity in interpretation.

Contrary to earlier some clinical reports from the interictal period (6, 12, 40, 62), the present findings do not display a significant deviation in the trend attributed to NAA, and the levels remained relatively consistent in the NTG versus saline injected rats, which is more in line with the majority of clinical $^1$H MRS migraine studies (16). NAA is widely held as a marker for neuronal and axonal integrity and is indicative of mitochondrial functioning as it is synthesized in neural mitochondria (12, 62). Physiologically, the changes in NAA seen in migraine and consequent mitochondrial disruption could be a result of long-term or repeated migraine. The current results appeared to indicate the absence of significant mitochondrial disturbance in NAA synthesis for this acute rat model, which permitted the use of NAA as an internal reference for the evaluation of other metabolites.

Likewise, acute NTG triggered rats did not demonstrate significant Cho alteration compared to saline controls in the current study, although Cho did decrease in both treatment groups over time. Constituting a less than 10% change from baseline for over 145 minutes for longitudinal acquisitions, the reason for this temporal Cho decrease in both groups is not well understood but would appear to be independent of either NTG or central sensitization. The total choline signal evaluated at 3.2 ppm is dominated by free choline, including less mobile upfield membrane cholines which could be remodeled over the hours of longitudinal acquisitions of this study. Interestingly, Valette *et al.* (63) and Boretius *et al.* (64) have indicated that choline containing compounds are impacted by the use of isoflurane. Using *in vivo* MRS, Valette *et al.* identified a relatively low choline apparent diffusion coefficient (ADC) compared to other *in vivo* metabolites, but an increased choline ADC (>50%) when increasing isoflurane from 1 to 2%. The low choline ADC was attributed to the confinement

of a large fraction of the total choline to a hindered intracellular compartment, and the increased ADC with isoflurane reduced this restriction, potentially related to increased permeability or membrane degradation (63). Boertius *et al.* indicated a reversible increase in choline signal with exposure to 1.75% isoflurane, attributed to the degradation of membrane-bound phosphatidylcholine (64). In fact, control data (Figure 4 of reference 64) displays a progressive decrease in total choline signal over a 130-min series of repeated *in vivo* MRS under continuous 1.75% isoflurane. This decrease over time is approximately 10%, which matches the Cho trend of the current study (Figure 5) for nearly the same level of anesthesia and timeframe of observation. Based on this supporting evidence, it is likely that isoflurane exposure increases the choline signal at 3.2 ppm resulting from its impact on the degradation of membrane-associated phosphatidylcholine or other choline compounds; over the course of longitudinal experiments spanning hours and prolonged isoflurane exposure, the increased free choline is recovered back to less mobile forms of choline (shifted away from 3.2 ppm) progressively, reflected in the significant time-dependent decrease in total Cho signal at 3.2 ppm for both NTG and saline groups. Most clinical studies of migraine do not identify a change in choline, although one study did identify decreased Cho levels between chronic migraine and control groups (13) during the interictal period, with the alterations attributed to membrane turnover resulting from choline's involvement in the synthesis of membrane constituents.

Although no clinical $^{1}$H MRS study of migraine has reported ictal findings to date (16), a single NTG study in rodents (15) has reported significant increases in Glu/GABA+ (+82%), tCr (+66%) and Cho (+67%) in the thalamus with a single acquisition 90 min after NTG treatment compared to saline controls. These increases are larger than any changes reported here and not consistent with the current findings. There are significant differences between this previous study and the current evaluation: data was acquired at 3 T from the thalamus utilizing a 10% chloral hydrate anesthetic; there was no baseline or pre-injected data reported; and data analysis references all metabolites (acquired with water-suppressed STEAM) to water (apparently acquired in a separate scan). With acquisition at a much lower field, the representative spectra from (15) demonstrate significantly less sensitivity and spectral resolution than what can be acquired at 21.1 T. As the data reported here was acquired in cortical regions versus the thalamic region of the previous study, these differences may reflect differential and more direct impacts of NTG on the trigeminovascular system.

It should be noted that any pre-clinical model of migraine is inherently imperfect given the extensive heterogeneity of migraine in the patient population. A potential limitation of the current study is the confounding effect of isoflurane anesthesia, although anesthetized controls provide a stable reference for the significant changes identified above. The analgesic impacts of isoflurane in this acute NTG model are not addressed or well known, and potentially may mask some biochemical changes related to pain perception.

## Conclusions

The present study is novel as it is the first time that metabolic substrates have been evaluated in the living brains of an acute rodent migraine model on a time course basis. Significant

changes in the concentrations of Lac, Tau and tCr along with increasing trends in Gly compared to controls suggest impaired metabolism as well as neuroprotective action with a temporal dependence related to onset of the migraine analogue. For this acute model, the changes in Lac (an early increase) and tCr (a decrease) suggest increased neural activity and/or altered glycolysis, which may be consistent with an altered sodium gradient across neural membranes and increased NKAT activity. The significantly increased Tau could be indicative of an endogenous neuroprotective and osmoregulatory action to maintain homeostasis, including NKAT activity. These metabolic alterations in the acute model would be important to investigate in chronic migraine or its models. Further investigations are warranted to understand the altered neural activity and metabolic dysregulation that follows the onset and sustained impacts of acute and chronic central sensitization and migraine.

## Supplementary Material

Refer to Web version on PubMed Central for supplementary material.

## Acknowledgments

This work was supported by the NIH (R01-NS072497 to MGH) and UCGP (to SCG) from the National High Magnetic Field Laboratory, which is funded by the NSF (DMR-1157490) and the State of Florida. The authors are extremely grateful to Drs. Lucio Frydman and Assaf Tal at the Weismann Institute for their expertise and guidance. The authors also wish to thank Aziz Ould Ismail and Ghoncheh Amouzandeh of Florida State University for their insights and help in reviewing this manuscript. Authors MGH and SCG contributed equally in the senior authorship of this paper.

## References

1. Steiner TJ, Birbeck GL, Jensen RH, Katsarava Z, Stovner LJ, Martelletti P. Headache disorders are third cause of disability worldwide. J Headache Pain. 2015 Jun 25.16:1–3. [PubMed: 25564352]
2. Parsons A, Strijbos P. The neuronal versus vascular hypothesis of migraine and cortical spreading depression. Curr Opin Pharmacol. 2003 Feb; 3(1):73–7. [PubMed: 12550745]
3. Harrington MG, Yang X, Cowan RP, Fonteh AN. Extracellular sodium increases neuron excitability in migraine. Neurology. 2009 Mar 17; 72(11):A175–-.
4. Harrington M, Fonteh A, Cowan R, Perrine K, Pogoda J, Biringer R, Huhmer A. Cerebrospinal fluid sodium increases in migraine. Headache. 2006 Jul-Aug;46(7):1128–35. [PubMed: 16866716]
5. Harrington MG, Chekmenev EY, Schepkin V, Fonteh AN, Arakaki X. Sodium MRI in a rat migraine model and a NEURON simulation study support a role for sodium in migraine. Cephalalgia. 2011 Sep; 31(12):1254–65. [PubMed: 21816771]
6. Dichgans M, Freilinger T, Eckstein G, Babini E, Lorenz-Depiereux B, Biskup S, Ferrari M, Herzog J, van den Maagdenberg A, Pusch M, et al. Mutation in the neuronal voltage-gated sodium channel SCN1A in familial hemiplegic migraine. Lancet. 2005 Jul 30; 366(9483):371–7. [PubMed: 16054936]
7. Arakaki X, Galbraith G, Pikov V, Fonteh AN, Harrington MG. Altered brainstem auditory evoked potentials in a rat central sensitization model are similar to those in migraine. Brain Res. 2014 May 14.1563:110–21. [PubMed: 24680742]
8. Ferrari LF, Levine JD, Green PG. Mechanisms mediating nitroglycerin-induced delayed-onset hyperalgesia in the rat. Neuroscience. 2016 Mar 11.317:121–9. [PubMed: 26779834]
9. Jansen-Olesen I, Tfelt-Hansen P, Olesen J. Animal migraine models for drug development: Status and future perspectives. CNS Drugs. 2013 Dec; 27(12):1049–68. [PubMed: 24234657]
10. Ashina M, Hansen JM, Olesen J. Pearls and pitfalls in human pharmacological models of migraine: 30 years' experience. Cephalalgia. 2013 Jun; 33(8):540–53. [PubMed: 23671251]

11. Bes A, Kunkel R, Lance JW, Nappi G, Pfaffenrath V, Rose FC, Schoenberg BS, Soyka D, Tfelt-Hansen P, Welch KMA, et al. The international classification of headache disorders, 3rd edition (beta version). Cephalalgia. 2013 Jul; 33(9):629–808. [PubMed: 23771276]
12. Sarchielli P, Tarducci R, Presciutti O, Gobbi G, Pelliccioli GP, Stipa G, Alberti A, Capocchi G. Functional 1H-MRS findings in migraine patients with and without aura assessed interictally. Neuroimage. 2005 Feb 15; 24(4):1025–31. [PubMed: 15670679]
13. Macri M, Garreffa G, Giove F, Ambrosini A, Guardati M, Pierelli F, Schoenen J, Colonnese C, Maraviglia B. Cerebellar metabolite alterations detected in vivo by proton MR spectroscopy. Magn Reson Imaging. 2003 Dec; 21(10):1201–6. [PubMed: 14725927]
14. Aguila MR, Lagopoulos J, Leaver AM, Rebbeck T, Huebscher M, Brennan PC, Refshauge KM. Elevated levels of GABA plus in migraine detected using H-1-MRS. NMR Biomed. 2015 Jul; 28(7):890–7. [PubMed: 25997981]
15. Ma Z, Wang S, Li C, Ma X, Gu T. Increased metabolite concentration in migraine rat model by proton MR spectroscopy in vivo and ex vivo. Neurol Sci. 2008 Oct; 29(5):337–42. [PubMed: 18941936]
16. Younis S, Hougaard A, Vestergaard MB, Larsson HB, Ashina M. Migraine and magnetic resonance spectroscopy: A systematic review. Curr Opin Neurol. 2017 Feb 24.
17. Reyngoudt H, De Deene Y, Descamps B, Paemeleire K, Achten E. H-1-MRS of brain metabolites in migraine without aura: Absolute quantification using the phantom replacement technique. Magn Reson Mat Phys Biol Med. 2010 Sep; 23(4):227–41.
18. Shemesh N, Dumez J, Frydman L. Longitudinal relaxation enhancement in H-1 NMR spectroscopy of tissue metabolites via spectrally selective excitation. Chem -Eur J. 2013 Sep 23; 19(39):13002–8. [PubMed: 24038462]
19. Shemesh N, Rosenberg JT, Dumez J, Muniz JA, Grant SC, Frydman L. Metabolic properties in stroked rats revealed by relaxation-enhanced magnetic resonance spectroscopy at ultrahigh fields. Nat Commun. 2014 Sep.5:4958. [PubMed: 25229942]
20. Iversen H, Olesen J, Tfelthansen P. Intravenous nitroglycerin as an experimental-model of vascular headache – basic characteristics. Pain. 1989 Jul; 38(1):17–24. [PubMed: 2506503]
21. Arakaki X, Foster H, Su L, Do H, Wain AJ, Fonteh AN, Zhou F, Harrington MG. Extracellular sodium modulates the excitability of cultured hippocampal pyramidal cells. Brain Res. 2011 Jul 15.1401:85–94. [PubMed: 21679932]
22. Fu R, Brey W, Shetty K, Gor'kov P, Saha S, Long J, Grant S, Chekmenev E, Hu J, Gan Z, et al. Ultra-wide bore 900 MHz high-resolution NMR at the national high magnetic field laboratory. J Magn Reson. 2005 Nov; 177(1):1–8. [PubMed: 16125429]
23. Qian C, Masad IS, Rosenberg JT, Elumalai M, Brey WW, Grant SC, Gor'kov PL. A volume birdcage coil with an adjustable sliding tuner ring for neuroimaging in high field vertical magnets: Ex and in vivo applications at 21.1 T. J Magn Reson. 2012 Aug.221:110–6. [PubMed: 22750638]
24. Rosenberg JT, Shemesh N, Muniz JA, Dumez J, Frydman L, Grant SC. Transverse relaxation of selectively excited metabolites in stroke at 21.1T. Magnetic Resonance in Medicine. 2016 n/a, n/a.
25. Garwood M, DelaBarre L. The return of the frequency sweep: Designing adiabatic pulses for contemporary NMR. J Magn Reson. 2001 Dec; 153(2):155–77. [PubMed: 11740891]
26. Wishart DS, Jewison T, Guo AC, Wilson M, Knox C, Liu Y, Djoumbou Y, Mandal R, Aziat F, Dong E, et al. HMDB 3.0-the human metabolome database in 2013. Nucleic Acids Res. 2013 Jan; 41(D1):D801–7. [PubMed: 23161693]
27. Watanabe H, Kuwabara T, Ohkubo M, Tsuji S, Yuasa T. Elevation of cerebral lactate detected by localized 1H-magnetic resonance spectroscopy in migraine during the interictal period. Neurology. 1996; 47(4):1093–5. [PubMed: 8857754]
28. Sandor P, Dydak U, Schoenen J, Kollias S, Hess K, Boesiger P, Agosti R. MR-spectroscopic imaging during visual stimulation in subgroups of migraine with aura. Cephalalgia. 2005 Jul; 25(7):507–18. [PubMed: 15955037]
29. Grimaldi D, Tonon C, Cevoli S, Pierangeli G, Malucelli E, Rizzo G, Soriani S, Montagna P, Barbiroli B, Lodi R, et al. Clinical and neuroimaging evidence of interictal cerebellar dysfunction in FHM2. Cephalalgia. 2010 May; 30(5):552–9. [PubMed: 19673908]

30. Lodi R, Lotti S, Cortelli P, Pierangeli G, Cevoli S, Clementi V, Soriani S, Montagna P, Barbiroli B. Deficient energy metabolism is associated with low free magnesium in the brains of patients with migraine and cluster headache. Brain Res Bull. 2001 Mar 1; 54(4):437–41. [PubMed: 11306197]

31. Barbiroli B, Montagna P, Cortelli P, Funicello R, Iotti S, Monari L, Pierangeli G, Zaniol P, Lugaresi E. Abnormal brain and muscle energy metabolism shown by 31P magnetic resonance spectroscopy in patients affected by migraine with aura. Neurology. 1992 Jun; 42(6):1209–14. [PubMed: 1603349]

32. Lodi R, Montagna P, Soriani S, Iotti S, Arnaldi C, Cortelli P, Pierangeli G, Patuelli A, Zaniol P, Barbiroli B. Deficit of brain and skeletal muscle bioenergetics and low brain magnesium in juvenile migraine: An in vivo P-31 magnetic resonance spectroscopy interictal study. Pediatr Res. 1997 Dec; 42(6):866–71. [PubMed: 9396571]

33. Schulz UG, Blamire AM, Corkill RG, Davies P, Styles P, Rothwell PM. Association between cortical metabolite levels and clinical manifestations of migrainous aura: An MR-spectroscopy study. Brain. 2007 Dec.130:3102–10. [PubMed: 17956910]

34. Welch K, Levine S, Dandrea G, Schultz L, Helpern J. Preliminary-observations on brain energy-metabolism in migraine studied by invivo P-31 nmr-spectroscopy. Neurology. 1989 Apr; 39(4): 538–41. [PubMed: 2927679]

35. Schurr A. Lactate: The ultimate cerebral oxidative energy substrate? J Cereb Blood Flow Metab. 2006 Jan; 26(1):142–52. [PubMed: 15973352]

36. Dienel GA. Brain lactate metabolism: The discoveries and the controversies. J Cereb Blood Flow Metab. 2012 Jul; 32(7):1107–38. [PubMed: 22186669]

37. Li B, Freeman RD. Neurometabolic coupling between neural activity, glucose, and lactate in activated visual cortex. J Neurochem. 2015 Nov; 135(4):742–54. [PubMed: 25930947]

38. Pellerin L, Magistretti P. Glutamate uptake into astrocytes stimulates aerobic glycolysis – a mechanism coupling neuronal-activity to glucose-utilization. Proc Natl Acad Sci U S A. 1994 Oct 25; 91(22):10625–9. [PubMed: 7938003]

39. Gilbert E, Tang JM, Ludvig N, Bergold PJ. Elevated lactate suppresses neuronal firing in vivo and inhibits glucose metabolism in hippocampal slice cultures. Brain Res. 2006 Oct 30.1117:213–23. [PubMed: 16996036]

40. Mohamed RE, Aboelsafa AA, Al-Malt AM. Interictal alterations of thalamic metabolic concentration ratios in migraine without aura detected by proton magnetic resonance spectroscopy. The Egyptian Journal of Radiology and Nuclear Medicine. 2013 Dec; 44(4):859–70.

41. Arngrim N, Schytz HW, Britze J, Amin FM, Vestergaard MB, Hougaard A, Wolfram F, de Koning PJH, Olsen KS, Secher NH, et al. Migraine induced by hypoxia: An MRI spectroscopy and angiography study. Brain. 2016 Mar 1.139:723–37. [PubMed: 26674653]

42. Becerra L, Veggeberg R, Prescot A, Jensen JE, Renshaw P, Scrivani S, Spierings ELH, Burstein R, Borsook D. A ‘complex’ of brain metabolites distinguish altered chemistry in the cingulate cortex of episodic migraine patients. NeuroImage-Clin. 2016; 11:588–94. [PubMed: 27158591]

43. Prescot A, Becerra L, Pendse G, Tully S, Jensen E, Hargreaves R, Renshaw P, Burstein R, Borsook D. Excitatory neurotransmitters in brain regions in interictal migraine patients. Mol Pain. 2009 Jun 30.5:34. [PubMed: 19566960]

44. Reyngoudt H, Paemeleire K, Dierickx A, Descamps B, Vandemaele P, De Deene Y, Achten E. Does visual cortex lactate increase following photic stimulation in migraine without aura patients? A functional H-1-MRS study. J Headache Pain. 2011 Jun; 12(3):295–302. [PubMed: 21301922]

45. Alfieri RR, Bonelli MA, Cavazzoni A, Brigotti M, Fumarola C, Sestili P, Mozzoni P, De Palma G, Mutti A, Carnicelli D, et al. Creatine as a compatible osmolyte in muscle cells exposed to hypertonic stress. J Physiol -London. 2006 Oct 15; 576(2):391–401. [PubMed: 16873409]

46. Beard E, Braissant O. Synthesis and transport of creatine in the CNS: Importance for cerebral functions. J Neurochem. 2010 Oct; 115(2):297–313. [PubMed: 20796169]

47. Erdelyi-Botor S, Aradi M, Kamson DO, Kovacs N, Perlaki G, Orsi G, Nagy SA, Schwarcz A, Doczi T, Komoly S, et al. Changes of migraine-related white matter hyperintensities after 3 years: A longitudinal MRI study. Headache. 2015 Jan; 55(1):55–70. [PubMed: 25319529]

48. Dandrea G, Cananzi A, Joseph R, Morra M, Zamberlan F, Milone F, Grunfeld S, Welch K. Platelet glycine, glutamate and aspartate in primary headache. Cephalalgia. 1991 Sep; 11(4):197–200. [PubMed: 1683816]
49. Rothrock J, Mar K, Yaksh T, Golbeck A, Moore A. Cerebrospinal-fluid analyses in migraine patients and controls. Cephalalgia. 1995 Dec; 15(6):489–93. [PubMed: 8706112]
50. Wesseldijk F, Fekkes D, Huygen FJPM, van de Heide-Mulder M, Zijlstra FJ. Increased plasma glutamate, glycine, and arginine levels in complex regional pain syndrome type 1. Acta Anaesthesiol Scand. 2008 May; 52(5):688–94. [PubMed: 18419723]
51. Martinez F, Castillo J, Leira R, Prieto J, Lema M, Noya M. Taurine levels in plasma and cerebrospinal-fluid in migraine patients. Headache. 1993 Jun; 33(6):324–7. [PubMed: 8349475]
52. Huxtable R. Physiological actions of taurine. Physiol Rev. 1992 Jan; 72(1):101–63. [PubMed: 1731369]
53. Timbrell J, Seabra V, Waterfield C. The in-vivo and in-vitro protective properties of taurine. Gen Pharmacol -the Vasc Syst. 1995 May; 26(3):453–62.
54. Tassorelli C, Joseph S, Nappi G. Neurochemical mechanisms of nitroglycerin-induced neuronal activation in rat brain: A pharmacological investigation. Neuropharmacology. 1997 Oct; 36(10): 1417–24. [PubMed: 9423929]
55. Birdsall TC. Therapeutic applications of taurine. Altern Med Rev. 1998 Apr; 3(2):128–36. 1998. [PubMed: 9577248]
56. Taranukhin AG, Taranukhina EY, Saransaari P, Podkletnova IM, Pelto-Huikko M, Oja SS. Neuroprotection by taurine in ethanol-induced apoptosis in the developing cerebellum. J Biomed Sci. 2010 Aug 24.17:S12. [PubMed: 20804586]
57. Moran J, Morales-Mulia M, Pasantes-Morales H. Reduction of phospholemman expression decreases osmosensitive taurine efflux in astrocytes. Biochim Biophys Acta-Mol Cell Res. 2001 Apr 23; 1538(2–3):313–20.
58. Harrington MG, Fonteh AN, Arakaki X, Cowan RP, Ecke LE, Foster H, Huehmer AF, Biringer RG. Capillary endothelial na plus, K plus, ATPase transporter homeostasis and a new theory for migraine pathophysiology. Headache. 2010 Mar; 50(3):459–78. [PubMed: 19845787]
59. Whittam R. Dependence of respiration of brain cortex on active cation transport. Biochem J. 1962; 82(1):205. [PubMed: 14006661]
60. Holopainen I, Liden E, Nilsson A, Sellstrom A. Depolarization of the neuronal membrane caused by cotransport of taurine and sodium. Neurochem Res. 1990 Jan; 15(1):89–94. [PubMed: 2325829]
61. Kanner B. Sodium-coupled neurotransmitter transport – structure, function and regulation. J Exp Biol. 1994 Nov.196:237–49. [PubMed: 7823025]
62. Zielman R, Teeuwisse WM, Bakels F, Van der Grond J, Webb A, van Buchem MA, Ferrari MD, Kruit MC, Terwindt GM. Biochemical changes in the brain of hemiplegic migraine patients measured with 7 tesla H-1-MRS. Cephalalgia. 2014 Oct; 34(12):959–67. [PubMed: 24651393]
63. Valette J, Guillermier M, Besret L, Hantraye P, Bloch G, Lebon V. Isoflurane strongly affects the diffusion of intracellular metabolites, as shown by H-1 nuclear magnetic resonance spectroscopy of the monkey brain. J Cereb Blood Flow Metab. 2007 Mar; 27(3):588–96. [PubMed: 16788716]
64. Boretius S, Tammer R, Michaelis T, Brockmoeller J, Frahm J. Halogenated volatile anesthetics alter brain metabolism as revealed by proton magnetic resonance spectroscopy of mice in vivo. Neuroimage. 2013 Apr 1.69:244–55. [PubMed: 23266699]

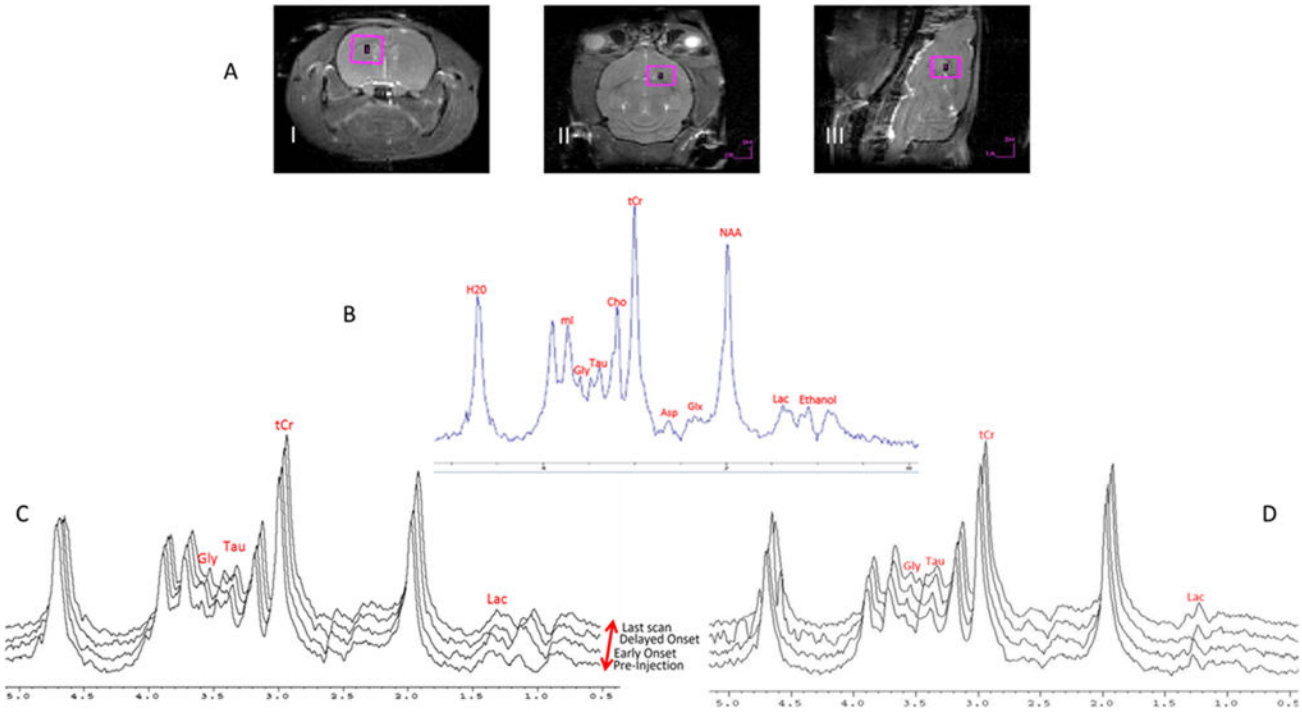


**Figure 1.**

A) Representative images demonstrate the 4×4×4-mm voxel placement in the i) coronal ii) axial and iii) sagittal anatomical directions. B) Representative *in vivo* 1D RE-MRS shows metabolite peak assignment. A TE = 52 ms for the RE-MRS spin-echo (TE = 64 ms including the LASER module) and TR = 2.5 s with 256 averages was used to achieve a total scan time of 10 min. C) Representative $^{1}$H metabolite spectra were acquired as time courses for a NTG-injected rat and D) saline-injected rat. For NTG, changes in Lac, Tau, tCr and Gly are evident compared to pre-injection baseline values; ethanol, as part of the NTG vehicle, is apparent after injection. The spectra have been plotted with sequential offsets in both frequency and vertical domains to better visualize the spectral time course.

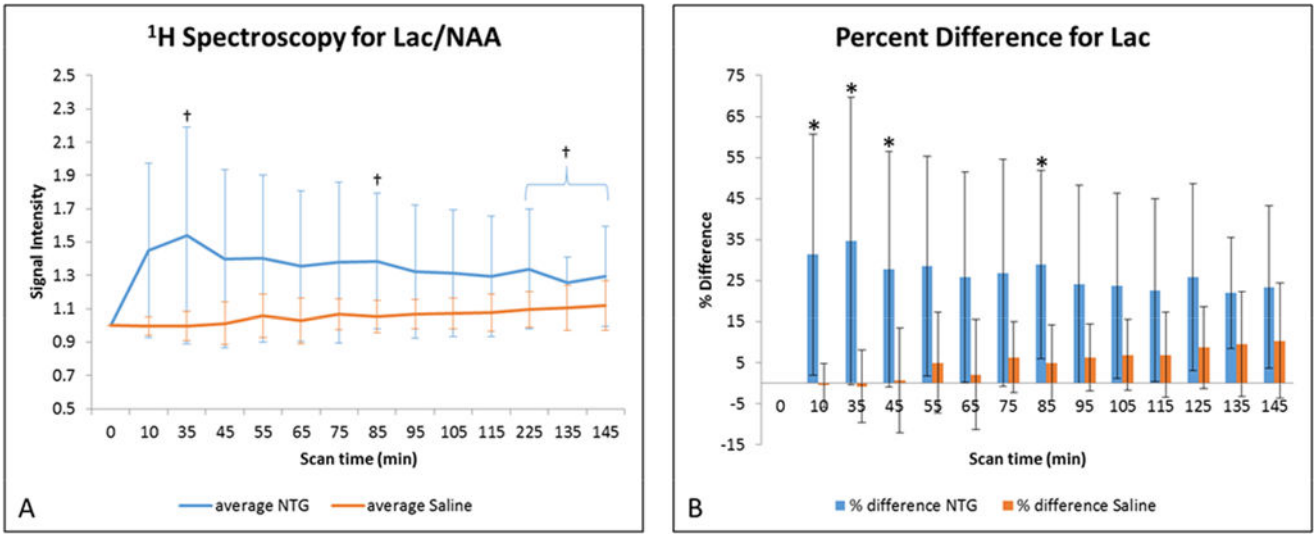


**Figure 2.**

A) Average lactate signal changes (mean ± SD) as a function of time after injection. Signals are normalized to NAA and pre-injection intensity values, with t=0 min representative of the pre-injection scan acquired just before IP injection. Statistical significances are †$p<0.05$ (LSD test) for temporal comparisons within NTG. (Blue error bars and brackets indicate NTG, whereas orange error bars indicate saline.) B) Percent difference in lactate (mean ± SD) with respect to the pre-injection value, with significance identified at *$p<0.05$ (Bonferroni's test) for comparisons between NTG and saline. Abbreviations: Lac, lactate; NAA, N-acetyl aspartate; IP, intraperitoneal; SD, Standard Deviation.

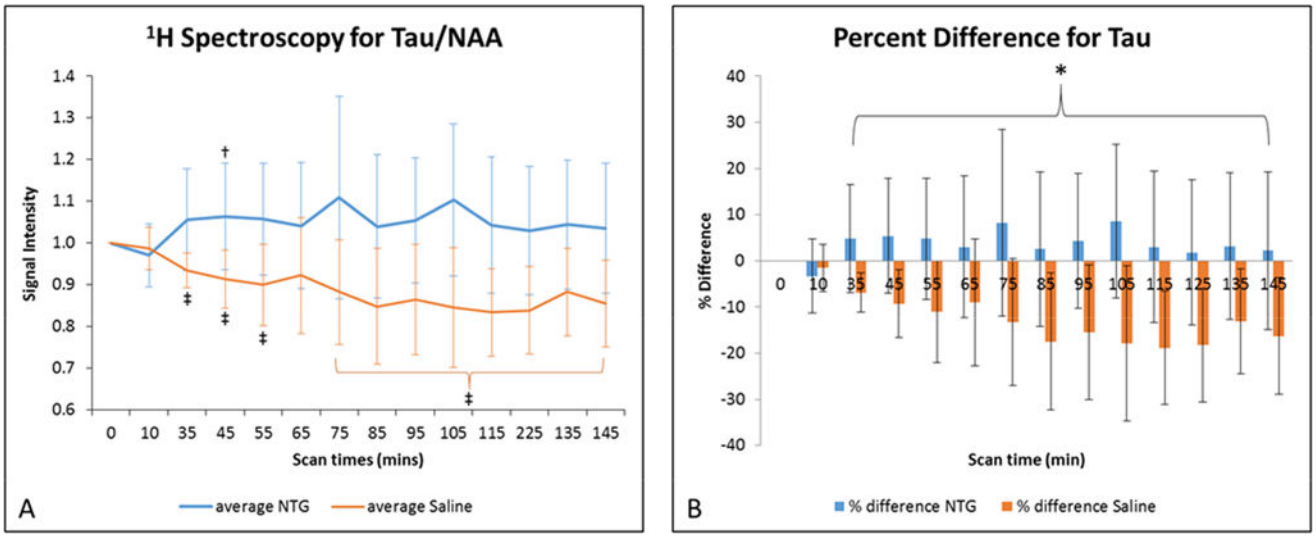


**Figure 3.**

A) Average taurine signal changes (mean ± SD) as a function of time after injection. Signals are normalized to NAA and pre-injection intensity values, with t=0 min representative of the pre-injection scan acquired just before IP injection. Statistical significances are †$p<0.05$ (LSD test) for temporal comparisons within NTG and ‡$p<0.05$ for comparisons within saline cohorts. (Blue error bars indicate NTG, whereas orange error bars and brackets indicate saline.) B) Percent difference in taurine (mean ± SD) with respect to the pre-injection value. Comparisons between NTG and saline are significant at *$p<0.05$ (Bonferroni's test). Abbreviations: Tau, taurine; NAA, N-acetyl aspartate; IP, intraperitoneal; SD, Standard Deviation.

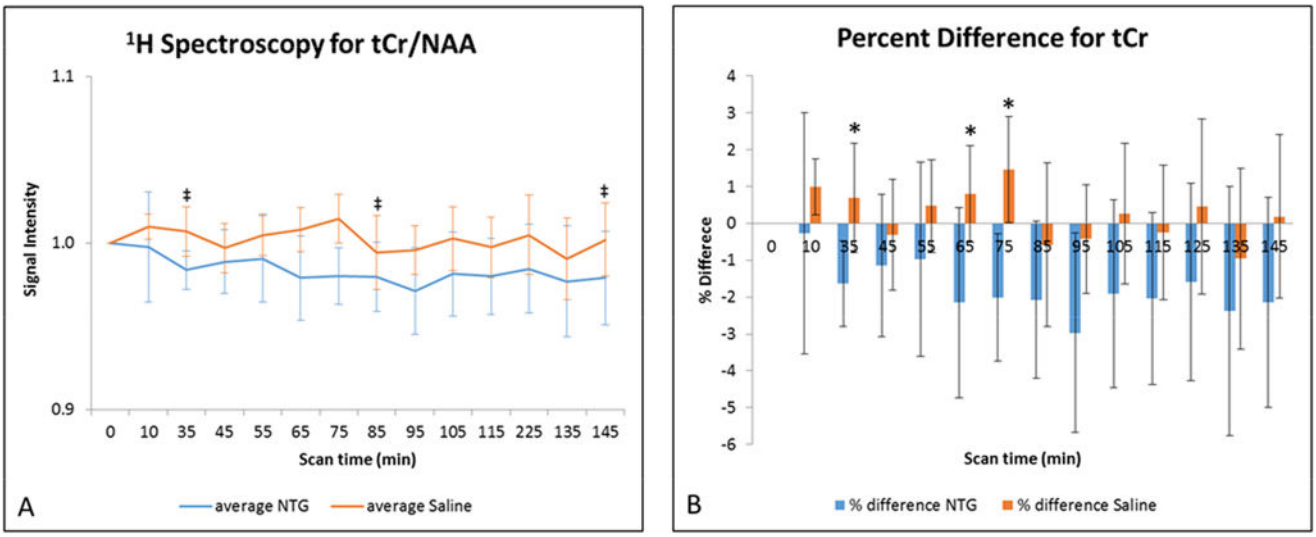


**Figure 4.**

A) Average total creatine signal intensities (mean ± SD) as a function of time after injection. Signals are normalized to NAA and pre-injection intensity values, with t=0 min representative of the pre-injection scan acquired just before IP injection. Statistical significances are ‡$p<0.05$ (LSD test) for temporal comparisons within saline cohorts. (Blue error bars indicate NTG, whereas orange error bars indicate saline.) B) Percent difference in total creatine (mean ± SD) with respect to the pre-injection value. Comparisons between NTG and saline are significant at *$p<0.05$ (Bonferroni's test). Abbreviations: tCr, total creatine; NAA, N-acetyl aspartate; IP, intraperitoneal; SD, Standard Deviation.

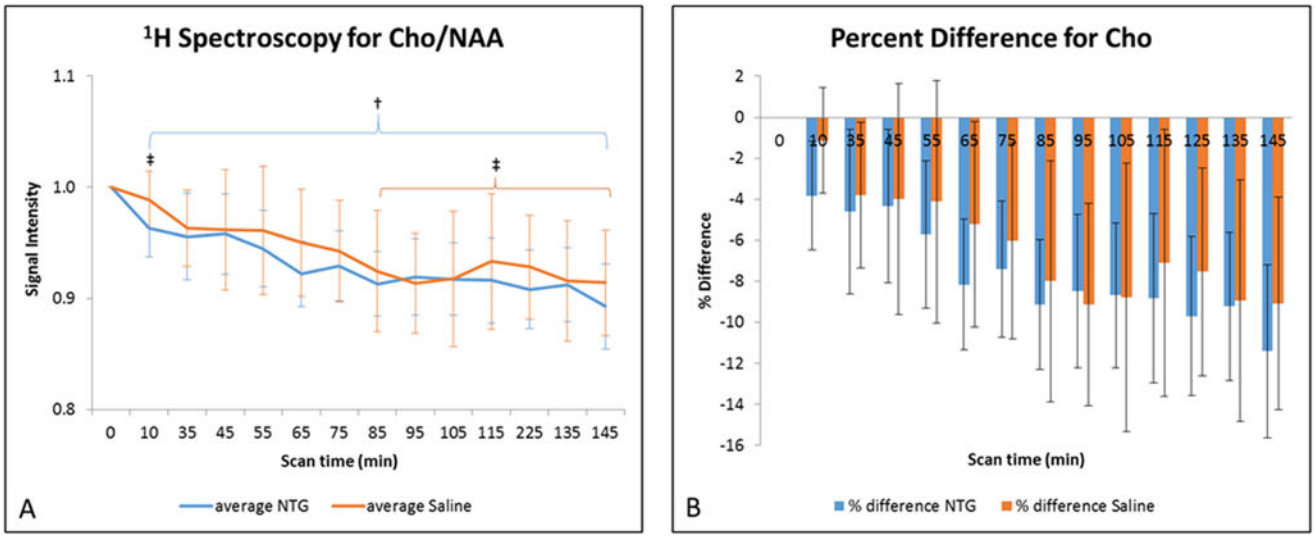


**Figure 5.**

A) Average choline signal intensities (mean ± SD) as a function of time after injection. Signals are normalized to NAA and pre-injection intensity values, with t=0 min representative of the pre-injection scan acquired just before IP injection. Statistical significances are †$p<0.05$ (LSD test) for temporal comparisons within NTG and ‡$p<0.05$ for comparisons within saline. (Blue error bars and brackets indicate NTG, whereas orange error bars and brackets indicate saline.) B) Percent difference in choline (mean ± SD) with respect to the pre-injection value. Comparisons between NTG and saline are significant at *$p<0.05$ (Bonferroni's test). Abbreviations: Cho, choline; NAA, N-acetyl aspartate; IP, intraperitoneal; SD, Standard Deviation.

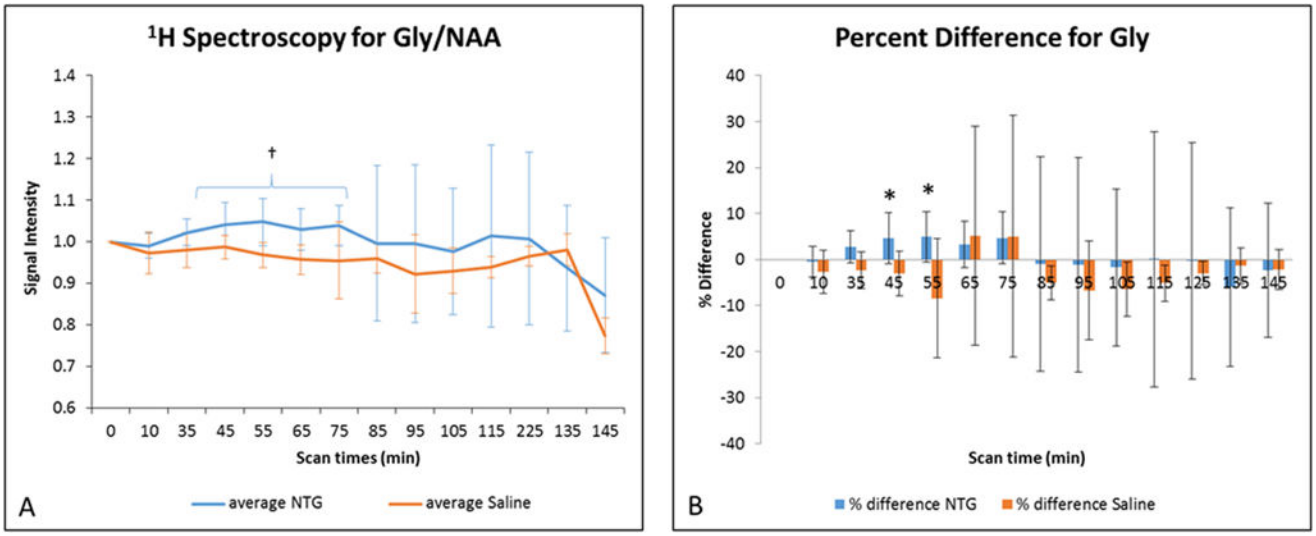


**Figure 6.**

A) Average Gly signal intensities (mean ± SD) as a function of time after injection. Signals are normalized to NAA and pre-injection intensity values, with t=0 min representative of the pre-injection scan acquired just before IP injection. Statistical significances are †$p<0.05$ (LSD test) for temporal comparisons within NTG. (Blue error bars and brackets indicate NTG, whereas orange error bars indicate saline.) B) Percent difference in Gly (mean ± SD) with respect to the pre-injection value. Comparisons between NTG and saline are significant at *$p<0.05$ (Bonferroni's test). Abbreviations: Gly, mixture of glycine, glutamine and glutamate; NAA, N-acetyl aspartate; IP, intraperitoneal; SD, Standard Deviation.